Title
Deep-water measurements of container ship radiated noise signatures and directionality.

Journal
Nature Energy, 142(3)

Authors
Gassmann, Martin
Hildebrand, John
Wiggins, Sean

Publication Date
2017-09-01

DOI
10.1121/1.5001063

Peer reviewed

Deep-water measurements of container ship radiated noise signatures and directionality

Martin Gassmann,[a] Sean M. Wiggins, and John A. Hildebrand
Scripps Institution of Oceanography, 9500 Gilman Drive, La Jolla, California 92093-0205, USA

(Received 1 February 2017; revised 31 July 2017; accepted 18 August 2017; published online 25 September 2017)

Underwater radiated noise from merchant ships was measured opportunistically from multiple spatial aspects to estimate signature source levels and directionality. Transiting ships were tracked via the Automatic Identification System in a shipping lane while acoustic pressure was measured at the ships' keel and beam aspects. Port and starboard beam aspects were 15°, 30°, and 45° in compliance with ship noise measurements standards [ANSI/ASA S12.64 (2009) and ISO 17208-1 (2016)]. Additional recordings were made at a 10° starboard aspect. Source levels were derived with a spherical propagation (surface-affected) or a modified Lloyd's mirror model to account for interference from surface reflections (surface-corrected). Ship source depths were estimated from spectral differences between measurements at different beam aspects. Results were exemplified with a 4870 and a 10 036 twenty-foot equivalent unit container ship at 40%–56% and 87% of service speeds, respectively. For the larger ship, opportunistic ANSI/ISO broadband levels were 195 (surface-affected) and 209 (surface-corrected) dB re 1 μPa^2 1 m. Directionality at a propeller blade rate of 8 Hz exhibited asymmetries in stern-bow (<6 dB) and port-starboard (<9 dB) direction. Previously reported broadband levels at 10° aspect from McKenna, Ross, Wiggins, and Hildebrand [(2012b). J. Acoust. Soc. Am. **131**, 92–103] may be ~12 dB lower than respective surface-affected ANSI/ISO standard derived levels.
 [http://dx.doi.org/10.1121/1.5001063]

[KGS] Pages: 1563–1574

I. INTRODUCTION

Underwater noise radiated from surface ships is a significant contributor to low-frequency ambient noise (<100 Hz) in the ocean (Wenz, 1962; Hildebrand, 2009). It is unintentionally generated by the ships' movement through the water and by the ships' auxiliary and propulsion machineries, in particular propellers (Urick, 1975; Ross, 1976). The cavitation processes occurring near the tip of the rotating propellers generate underwater noise both over a broad frequency range and at a series of distinct frequencies that correspond to the propeller blade rate and its harmonics (Gray and Greeley, 1980). Relating these and other features of underwater radiated noise from a ship, often called its signature, to naval-architectural and operational (e.g., draft and speed) parameters is an ongoing research effort, e.g., Wittekind (2014).

Given the high intensity of ship underwater radiated noise at frequencies at which absorption and scattering of sound in water is small (<10^{-2} dB/km), ships are being increasingly considered as an opportunistic sound source, e.g., for acoustic tomography (Cornuelle *et al.*, 2016; Kuperman *et al.*, 2017) and for estimating seafloor properties (Knobles, 2015) or the acoustic waveguide invariant (Verlinden *et al.*, 2017). On the other hand, environmental concerns about the noise contributions from shipping have been raised, e.g., Redfern *et al.* (2017).

To study the radiated noise levels of modern commercial ships, McKenna *et al.* (2012b) conducted opportunistic measurements in the Santa Barbara Channel with a single hydrophone for a large number of ships at their starboard beam aspect of approximately 10°, while relying on data from the automatic identification system (AIS) for the tracks, speeds, and identifications of passing ships. A similar opportunistic study has been conducted at an even shallower measurement aspect of about 0.2° by Veirs *et al.* (2016) in the Haro Strait, Washington. Source levels were found to be 5–10 dB lower than McKenna *et al.* (2012b) while the differences could not be explained by Veirs *et al.* (2016).

Besides opportunistic studies that measure large numbers of ships at a single aspect, more extensive measurements are available for a smaller number of ships that cooperated in controlled experiments. For example, underwater noise of a coal carrier built in 1977 was measured during multiple measurement runs at a testing facility of the U.S. Navy by Arveson and Vendittis (2000). These measurements suggest a significant aspect-dependence of source levels that is illustrated in radiation patterns. An aspect-dependence of source levels has also been observed for a small hydrographic survey vessel (560 tons, 40 m length) by Trevorrow *et al.* (2008). Given the aspect-dependence of ships' underwater radiated noise, current standards for ship noise measurements, ANSI/ASA S12.64-2009 (Grade A and B) and ISO 17208-1:2016, require measurements at beam aspects of 15°, 30°, and 45° on the ships' port and starboard-side to facilitate comparisons between measurements that were conducted in accordance with the standards (ANSI/ASA, 2009; ISO 2016). Despite averaging over multiple beam aspects, the Grade A and B "source levels" of the ANSI/ASA and the "radiated noise levels" of the ISO

[a]Electronic mail: martin.gassmann044@gmail.com

standard remain affected by propagation effects such as interference from surface reflections (ANSI/ASA, 2009; Brooker and Humphrey, 2016; ISO, 2016) and will be henceforth referred to as surface-affected ANSI/ISO source levels. The remaining, unaccounted interference effects from surface reflection in the surface-affected ANSI/ISO source levels impede their potential use in propagation modeling and comparisons with opportunistic measurements at shallower aspects, e.g., McKenna *et al.* (2012b), Jansen and de Jong (2015), and Veirs *et al.* (2016).

In this study, underwater noise radiation patterns of contemporary merchant ships were measured opportunistically in a shipping lane in 585 m deep water at all standard-required beam aspects (15°, 30°, and 45°) in addition to keel and a 10° starboard aspect. This facilitates a comparison of surface-affected ANSI/ISO source level estimates with single-aspect source levels from keel and the location of previous measurements from McKenna *et al.* (2012b). To better account for interference from surface reflection, surface-corrected source levels were derived in addition. Results are exemplified with the *CSCL South China Sea* (IMO 9645920), a 10 036 twenty-foot equivalent unit (TEU) container ship that transited at 20.4 knots with a draft of 9.6 m. To illustrate the variability of ship noise, source level estimates for two passages of the *MSC Monterey* (IMO 9349796), a container ship with about half the capacity of the *CSCL South China*, are also considered.

II. METHODS

A. Experimental setup

In December 2015, eight high-frequency acoustic recording packages (HARPs) (Wiggins and Hildebrand, 2007) were deployed at four sites in the Santa Barbara Channel in the Southern California Bight (Fig. 1). Three of the four sites (PORT, KEEL, and STBD) were in the 1 nm (1.852 km) wide northbound lane for merchant ships that transit from the ports of Los Angeles and Long Beach through the Santa Barbara Channel. The fourth site (B) was 3.18 km off the northbound shipping lane's centerline at a location that was previously used for measuring underwater ship noise (McKenna *et al.*, 2012a, 2012b, 2013). At all four sites the water depth was 585 m due to their proximity to the center of the Santa Barbara Basin.

The sites PORT, KEEL, and STBD were chosen to opportunistically measure the underwater radiated noise from northward traveling ships at their port, keel, and starboard aspects, respectively [Figs. 1(b) and 2]. At each of these three sites one subsurface mooring was deployed. The mooring at site KEEL carried a single HARP with a hydrophone at a depth of 565 m. At sites PORT and STBD, each mooring was equipped with three HARPs at 151, 326, and 565 m depth to yield the inclination angles of 15°, 30°, and 45° at the closest point of approach (CPA) in compliance with ANSI/ASA (2009) and ISO (2016) (Table I). In addition, an accelerometer for monitoring all three spatial dimensions (OpenTag, Loggerhead Instruments Inc., Sarasota, FL) was attached to the top of the PORT and STBD moorings at

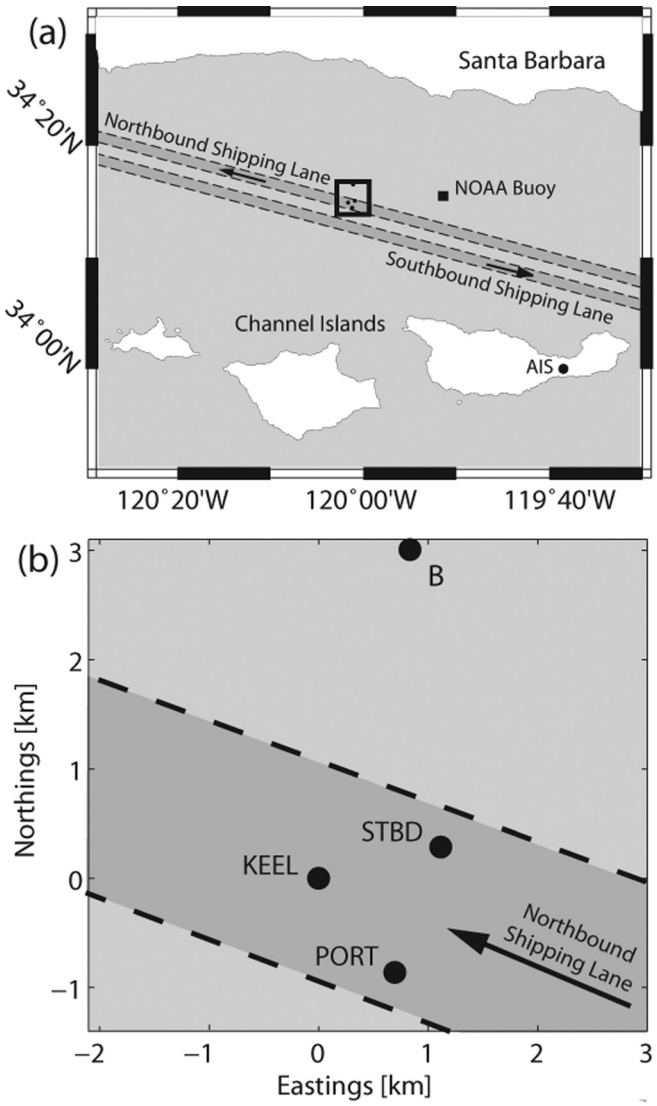

FIG. 1. (Color online) (a) Location of acoustic measurement site (box) near the Channel Islands in the Southern California Bight. Shipping lanes are shown in dark gray with black dashed lines. Direction of travel in shipping lanes is indicated by arrows. Locations of weather buoy (NOAA Station 46053) and AIS receiver are represented by a black square and circle, respectively. (b) Map showing mooring locations (PORT, KEEL, and STBD) in the northbound shipping lane (dark gray with dashed lines) and location of a single acoustic seafloor recorder (B) located at the site used by McKenna *et al.* (2012a, 2012b, 2013). Map is geo-referenced to mooring KEEL (34° 14.906′ N 120° 1.655′ W).

128 m depth to monitor potential drifts of the hydrophones due to possible ocean currents bending of the mooring. As the estimated bending angles of both mooring cables did not exceed 5° during the ship passages, hydrophone position drifts were considered negligible (ANSI/ASA, 2009). At site B, a single HARP with a hydrophone depth of 565 m was deployed as a seafloor package similarly to the experiment described in McKenna *et al.* (2012a, 2012b, 2013). The inclination angle to the center of the shipping lane at site B was 10.4°.

Acoustic data were collected continuously by all HARPs at a sampling frequency of 200 kHz for 39 days. The location of each mooring (Table I) was derived from the travel times of pings sent from a surface ship at known GPS-derived

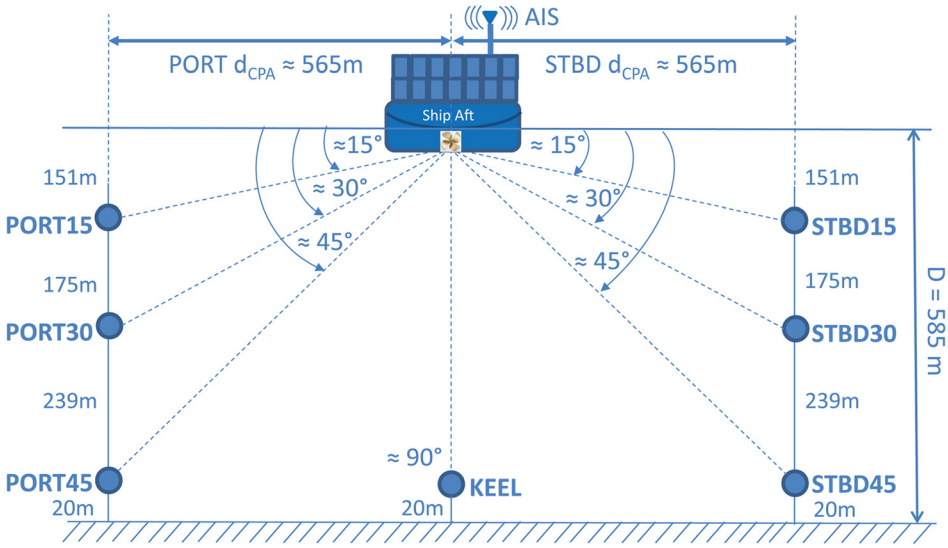

FIG. 2. (Color online) Cross-sectional view of the northbound shipping lane showing the hydrophone array (circles) with respect to a container ship (traveling into the page) in 585 m deep water. Hydrophone moorings are located portside (PORT), underneath (KEEL), and starboard-side (STBD) with respect to the transiting ship and are at least 565 m apart from each other when measured transversely to the ships' direction of travel. Hydrophones of mooring PORT (PORT15, PORT30, and PORT45) and STBD (STBD15, STBD30, and STBD45) are located at 151, 326, and 565 m depth, respectively, which corresponds approximately to the inclination angles of 15°, 30°, and 45° [ANSI/ASA (2009) and ISO (2016)]. Mooring KEEL has a single hydrophone at an approximate aspect of 90°. Ships are identified and tracked from their transmitted AIS information.

locations and times, to the transponder of each mooring's release system (Wiggins *et al.*, 2013). The root-mean-squared position errors of the least-square algorithm were smaller than 5 m. The pings sent to the transponders were also received by the hydrophones and their measured one-way travel times were utilized to verify the time-synchronization of all HARPs with an accuracy of less than 5 msec. In addition, drift rates of the HARPs' clocks were measured before and after the deployment and ranged from 9.38×10^{-11} (KEEL) to 3.12×10^{-9} (PORT15). Hydrophone sensitivities and transfer function calibrations of HARPs were performed at the Scripps Whale Acoustics Laboratory and at the U.S. Navy's Transducer Evaluation Center facility in San Diego, California.

Ships were identified and tracked by an AIS receiver located on Santa Cruz Island (33° 59.667′ N and 119° 37.941′ W), providing coverage for both shipping lanes and their vicinity. The received AIS messages were continuously logged on-site by a computer that was time-synchronized via the internet. AIS messages were decoded with the Shipplotter program (ver. 12.4.6.5 COAA) and software developed by Robin T. Bye (Project: Virtual More) to infer information for each passing ship including its identification (IMO number), position (latitude and longitude), ship's reference point for the reported position, Speed Over Ground (SOG), draft (maximum present static draft), and destination.

TABLE I. Locations and depths of the HARPs.

HARP site name	Latitude [North]	Longitude [West]	Hydrophone depth [m]
B	34° 16.532′	120° 1.112′	565
STBD15	34° 15.061′	120° 0.930′	151
STBD30	34° 15.061′	120° 0.930′	326
STBD45	34° 15.061′	120° 0.930′	565
KEEL	34° 14.906′	120° 1.655′	565
PORT15	34° 14.440′	120° 1.202′	151
PORT30	34° 14.440′	120° 1.202′	326
PORT45	34° 14.440′	120° 1.202′	565

The positions and SOGs for each ship passage were received mostly every 12 s and interpolated to achieve a time-resolution of 3 s. Additional information that was not provided by AIS, such as details regarding the ship's propulsion system, was retrieved from Lloyd's Register of Ships (IHS, 2016/2017 edition).

During each ship passage the direction, height, and average period of the ocean waves as well as the speed and direction of the wind were measured by a National Oceanic and Atmospheric Administration (NOAA) buoy at 34° 15.150′ N and 119° 51.200′ W (station 46053) [Fig. 1(a)]. These data were collected and made freely available by NOAA/NDBC (National Oceanic and Atmospheric Administration/National Data Buoy Center, http://www.ndbc.noaa.gov/). In addition, temperature and salinity profiles were measured near site B at 34° 16.640′ N and 120° 1.769′ W by the California Cooperative Oceanic Fisheries Investigations (CalCOFI, http://calcofi.org/data.html) program (line 81.8 and station 46.9) on January 18 and 19, 2016 approximately 8 h before the passage of the *CSCL South China Sea*. A sound speed profile was inferred from the measured salinity and temperature profiles (Roquet *et al.*, 2015) with a harmonic mean sound speed, c_{hm}, of 1490 m/s. The sound speed near the sea surface and the seafloor was 1505 and 1486 m/s, respectively, and the profile was generally downward refracting except for a subsurface isovelocity layer of 1504 m/s between 13 and 39 m depth.

B. Data processing

The acoustic data were processed to estimate the sound pressure levels of the underwater sound in the time-frequency domain. By accounting for losses in sound transmission over the known distances between the ship and the HARPs, estimates for source levels of the ships' underwater radiated noise were obtained.

To minimize interference from other sound sources than the ship under investigation, the following conditions were met during any of the transits: (i) absence of other ship(s) in the acoustic data and in AIS data within an area of 567 km^2,

(ii) absence of any other man-made sound sources in the bandwidth of interest (5–20 000 Hz), and (iii) no violation of nominal environmental conditions required by ANSI/ASA (2009) and ISO (2016) such as excessive wave height and wind speed ($>10.28\,\mathrm{ms}^{-1}$).

1. RLs

Each of the eight pressure time series was divided into consecutive, non-overlapping segments with a length of 1 s (200 000 samples). A two-sided Fast Fourier Transform (FFT) with NFFT = 200 000 points was applied to each segment to yield a frequency bin spacing of 1 Hz. The magnitude squared values of the complex FFT coefficients for the positive frequencies were multiplied by $2/\mathrm{NFFT}^2$ to account for the processing gain of the FFT. Their mean was computed over a time interval of 5 s (five sets of coefficients) every 3 s to smooth the resulting time-frequency distribution ($|\overline{\mathrm{FFT}}|^2$). The squared received sound pressures for each HARP were reported on a relative logarithmic scale in decibels (dB) with a reference pressure of 1 μPa^2 and are referred to as received levels (RLs):

$$\mathrm{RL} = 10\log_{10}\left(\frac{|\overline{\mathrm{FFT}}|^2}{(1\,\mu\mathrm{Pa})^2}\right). \tag{1}$$

The time-frequency distribution of RL will be henceforth referred to as a spectrogram.

2. TL

The loss in sound transmission between the radiating ship and the receiving hydrophones was modelled by reducing the complex horizontal and vertical source distribution of a ship to a single point source with an effective source depth. To further allow for comparison of source levels to previous studies (Arveson and Vendittis, 2000; McKenna *et al.*, 2012a, 2012b, 2013) and for compliance with ANSI/ASA (2009) and ISO (2016), the transmission loss (TL) was modeled as spherical spreading over the slant range, r, in meters,

$$\mathrm{TL_{SS}} = 10\log_{10}(r/1\,\mathrm{m})^2. \tag{2}$$

For computing r, the reference point of the ship was defined to be halfway between the propeller and the engine room for all frequencies (ANSI/ASA, 2009). For each ship location, this reference point was derived from the AIS-reported reference point for position reporting.

In addition, the TL was computed by using RAMSGEO (version 0.5C01.01.01), a parabolic equation (PE) model for multi-layer, elastic seafloors that uses a split-step Padé algorithm that was provided by the Centre for Marine Science and Technology at Curtin University (Collins, 1993). Modeling was carried out for a single point source with eight Padé terms and a spatial resolution of 1 m (horizontally and vertically) up to a range of 3.5 km. The environment is further defined by a flat sea surface and a flat seafloor at a depth of 585 m independent of range and azimuth. The CalCOFI-derived sound speed profile was used to characterize the water column, while the compressional wave speed and density profiles for the sub-seafloor were obtained from the Integrated Ocean Discovery Program's drilling data that were collected at site 893 Hole A in the Santa Barbara Channel (Carson *et al.*, 1992). The seafloor shear wave speed profile was inferred from the dispersion of interface waves measured during the Thumper experiment in the Southern California Bight (Table I in Nolet and Dorman, 1996). All profiles were assumed to be independent of azimuth and range. Narrowband TLs were modelled for frequencies between 4.5 and 1000.5 Hz in increments of 0.5 Hz. A moving average filter with a window of 1 Hz (<1 km range) or 3 Hz (>1 km range) was applied to smooth the frequency-dependent TL for the range-depth point of each hydrophone. The TL was then down-sampled in frequency by a factor of 2 to yield a resolution of 1 Hz for integer frequency bins.

Alternatively, TL was also modeled as an image-interference (Lloyd's mirror) by ignoring sound refraction and the sea bottom to account solely for the reflections from a flat sea surface

$$\mathrm{TL_{LM}} = 10\log_{10}\left(\frac{(r/1\,m)^2}{2\left(1-\cos\left(\frac{4\pi f z_s z_r}{c_{\mathrm{hm}} r}\right)\right)}\right), \tag{3}$$

where f represents the sound frequency in Hz, and z_s and z_r are the source and hydrophone depth in meters, respectively (Urick, 1975).

A comparison of the three TL models for source depths of 1, 3, and 5 m is shown for PORT45/STBD45 [Fig. 3(a)] and PORT15/STBD15 [Fig. 3(b)] with ranges approximately equal to the water depth, in addition to site B [Fig. 3(c)] with ranges approximately equal to 5.5 times the water depth. Source depths were chosen to sample the range of approximate propeller tip depths in which underwater noise due to cavitation is being generated and radiated (Gray and Greeley, 1980). Due to significant mismatches between the interference lobes present in the recordings and the interference lobes suggested by the PE and Lloyd's mirror model, neither of the two models was selected. Rather, a combination of the Lloyd's mirror and the spherical spreading model was used as an alternative for the pure spherical spreading model in order to account for the surface-induced, source depth-dependent increase in TL with decreasing frequency without introducing mismatched interference lobes. In this TL model, the Lloyd's mirror model was used from 5 Hz up to the lowest frequencies at which the Lloyd's mirror model had the same TL as the spherical spreading model. At greater frequencies, the spherical spreading model was used. This TL model will be herein referred to as the modified Lloyd's mirror model.

3. Effective source depth for ship noise

The effective source depth of the underwater radiated noise from each transiting ship was estimated by minimizing the difference between the spectral difference in the measured TL and the spectral difference of the modelled TL at various source depths for a pair of hydrophones at two separate

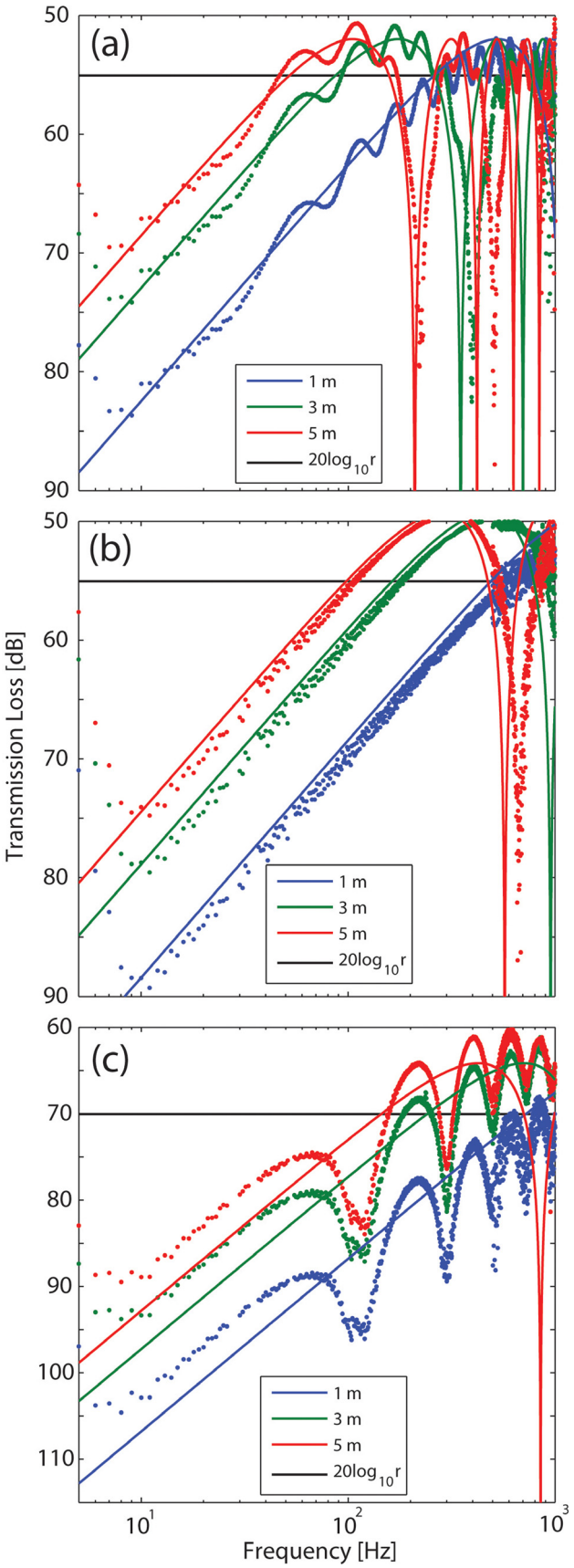

FIG. 3. (Color online) Comparison of TL models for (a) STBD45/PORT45, (b) STBD15/PORT15, and (c) Site B for frequencies between 5 and 1000 Hz. PE model (dots) and Lloyd's mirror model (lines) are shown for source depths of 1 m (blue), 3 m (green), and 5 m (red). Spherical spreading model for near-surface source depths (<10 m) is indicated by black lines.

inclination angles (Trevorrow *et al.*, 2008). Assuming that the spectral differences in the measured RL are mostly due to differences in TL rather than due to potential asymmetries of the source, the depth at which the spectral difference in the modelled TL best matches the spectral differences of the corresponding RL, yields the effective source depth:

$$\min\{|(RL_{45^\circ}-RL_{15^\circ})-(TL_{45^\circ}-TL_{15^\circ})|^2\}. \quad (4)$$

To demonstrate the feasibility of the technique for ANSI/ISO measurement campaigns, the 15° and 45° hydrophones have been selected, respectively, to obtain the effective source depth of each transiting ship. The spectral difference in the TL was computed for the pairs STBD15–STBD45 and PORT15–PORT45 with the modified Lloyd's mirror model for source depths of 1, 3, 5, and 10 m.

For comparison, a ship's effective source depth was also computed from the AIS-reported maximum present static draft during its passage minus 85% of its estimated propeller diameter (Gray and Greeley, 1980). The diameter and keel offset of the single, fixed-pitch propellers were estimated from photos taken at the ship's stern aspect while in dry dock and by considering the propulsion power and speed of the ship engine (MAN Diesel & Turbo, Augsburg, Germany, http://marine.man.eu/propeller-aft-ship/basic-principles-of-propulsion).

4. Source levels

The levels of the squared pressure from the underwater radiated noise from ships at a reference distance of 1 m, source levels (SLs), were inferred from the RLs by accounting for losses in sound transmission (TLs) between the ship and each HARP,

$$SL = RL + TL. \quad (5)$$

With the spherical spreading model and with the modified Lloyd's mirror model, surface-affected and surface-corrected source levels were computed, respectively, (1) at the aspect of site B with an inclination angle of 10° (Site B), (2) by averaging over the port and starboard beam aspects with inclination angles of 15°, 30°, and 45° (ANSI/ISO), and (3) at the keel aspect with an inclination angle of 90° (KEEL).

For Site B, surface-affected and surface-corrected source levels were derived for each passage from averaging the RLs within a data window period that is defined by the time it takes the ship to travel 1.5 times its own length with respect to the CPA, as described in McKenna *et al.* (2012b). Estimates of ANSI/ISO source levels for each ship were derived from a single, opportunistic passage [equivalent to two measurement runs in ANSI/ASA (2009) and ISO (2016)] by averaging over the port and starboard beam aspects of 15°, 30°, and 45° according to Eqs. (8) and (9) from ANSI/ASA (2009) utilizing the RLs from hydrophones PORT15, PORT30, PORT45, STBD15, STBD30, and STBD45. The data window period for each of these six HARP recordings was derived from Eq. (2) from ANSI/ASA (2009) with the required azimuthal data window angle of ±30°. The resulting signature source levels in 1 Hz bins were also expressed in 1/3 octave bands to comply with ANSI/ASA (2009). For KEEL, the source levels were

TABLE II. Characteristics of ships under investigation. Asterisks indicate estimated values.

Name	*CSCL South China Sea*	*MSC Monterey*
IMO number	9645920	9349796
Maximum capacity [TEU]	10 036	4870
Year built	2014	2007
Service speed	23.5 knots ($12.1\,ms^{-1}$)	24.0 knots ($12.3\,ms^{-1}$)
Maximum draft [m]	15.000	13.400
Length [m]	335.00	274.98
Width [m]	48.60	32.30
Engine type	Mitsui/MAN-B&W 10S90ME-C9	Doosan/MAN-B&W 7K98MC-C
Engine power [kW]	58 100	39 970
Number of cylinders	10	7
Propeller diameter [m]	7.5*	5.8*
Number of propeller blades	6*	5*

estimated for each ship passage by averaging the RLs from KEEL within a data window period that is defined by the time it takes the ship to transit over site KEEL bow to stern.

Broadband source levels were computed in the frequency range from 5 Hz to 1 kHz.

5. Radiation patterns

Each source level estimated at a given time was associated with a ship location based on the ship's trajectory. For each location of a ship's trajectory, the known positions of the HARPs can be represented in a spherical coordinate system that is centered at the ship's reference point. In this spherical coordinate system the directions from the ship's reference point toward the bow, starboard, stern, and port aspect coincide with an azimuthal angle of 0°, 90°, 180°, and 270°, respectively, while the keel aspect (directly below the ship's reference point) corresponds to an inclination angle of 90° (Arveson and Vendittis, 2000). The positions of the HARPs were azimuthal-equidistantly projected onto a lower half-sphere with a radius of 1 m to associate the azimuthal and inclination angle to each HARP with its source level using the Generic Mapping Tools (Wessel *et al.*, 2013). Assuming that the received underwater noise at all frequencies was solely radiated from the ship's reference point, frequency-dependent radiation patterns of the underwater source levels were generated for each ship that transits by the measurement sites.

III. RESULTS

Underwater noise levels and radiation patterns are presented for the *CSCL South China Sea* (IMO 9645920), a 10 036 TEU container ship with a length of 335 m (Table II). She will be henceforth also referred to as the M/V SCS. Measurements of the M/V SCS were taken at 20.4 knots (87% of her service speed) and at a draft of 9.6 m on January 19, 2016. Source levels from the transit of the M/V SCS were compared with two slower transits of a ship with about half the container capacity, the *MSC Monterey* (IMO 9349796) (Tables II and III). The *MSC Monterey* will be henceforth also referred to as the M/V MONT.

A. RLs of the M/V SCS

The spectrograms of the received sound pressure levels for all HARPs are shown on a linear time and frequency scales for a duration of 30 min in which the M/V SCS traveled 18.9 km (Figs. 4 and 5). All spectrograms begin at 8:40 GMT on January 19, 2016. The RLs for the HARPs in the shipping lane ranged typically between 60 and 140 dB re $1\,\mu Pa^2$ in 1 Hz bins for frequencies of up to 500 Hz (Fig. 4). At the distant site B, RLs were overall lower and typically between 50 and 124 dB re $1\,\mu Pa^2$ (Fig. 5). The highest RLs were found in the vicinity of the respective CPA at approximately 15 min when the ship's azimuth is about 0° [Figs. 4(a)–4(f) and 5] or its inclination angle is about 90° for KEEL [Fig. 4(g)]. Overall the received sound pressure levels were higher at depths with a greater inclination angle [e.g., 15° in Figs. 4(a) and 4(d) versus 90° in Fig. 4(g)]. "U" shaped interference patterns caused by surface and bottom reflections were visible in all spectrograms. Despite the unique features of each interference pattern, there is a higher degree of similarity between them at the same inclination angle [e.g., at 15° in Figs. 4(a) and 4(d)] than at different inclination angles [e.g., at 15° and 45° in Figs. 4(a) and 4(c)]. In addition, all spectrograms exhibited lines of nearly constant frequency, which correspond to tonals generated by the ship' rotating machinery. Due to the movement of the ship, the frequency lines are Doppler-shifted; most notably at the higher frequencies (e.g., shift >1 Hz at $f > 142$ Hz).

B. Effective source depth of M/V SCS

The effective source depth during the passage of the M/V SCS was found to be between 1 and 5 m with 3 m being the best fit to the distribution of the difference in RL for hydrophone pair STBD15–STBD45 with a root-mean-square error (RMSE) of 3.2 dB (Fig. 6). The source depth of 3 m was likewise observed as the best fit for the hydrophone pair PORT15–PORT45 (RMSE = 3.4 dB) and was found to be consistent within less than 0.5 m with the source depth that was derived from the propeller diameter (Table II) and AIS-reported draft during M/V SCS passage (Table III) according to Gray and Greeley (1980).

C. Source levels of the M/V SCS

The source levels computed with the spherical spreading loss model [Eq. (2)] for the M/V SCS were found to be the highest mostly for KEEL, slightly lower for ANSI/ISO, and significantly lower for Site B low aspect angle with broadband source levels of 197, 195, and 182 dB re $1\,\mu Pa^2$ @ 1 m, respectively [Fig. 7(a)]. The broadband source level estimate from Site B agrees within 2–3 dB with the majority of source levels of container ships that were measured at similar speeds at this site during a previous study (McKenna *et al.*, 2012b).

The significant difference of 13 to 15 dB in source levels at frequencies below 100 Hz between Site B and ANSI/ISO and KEEL was reduced to 3–7 dB when surface reflections

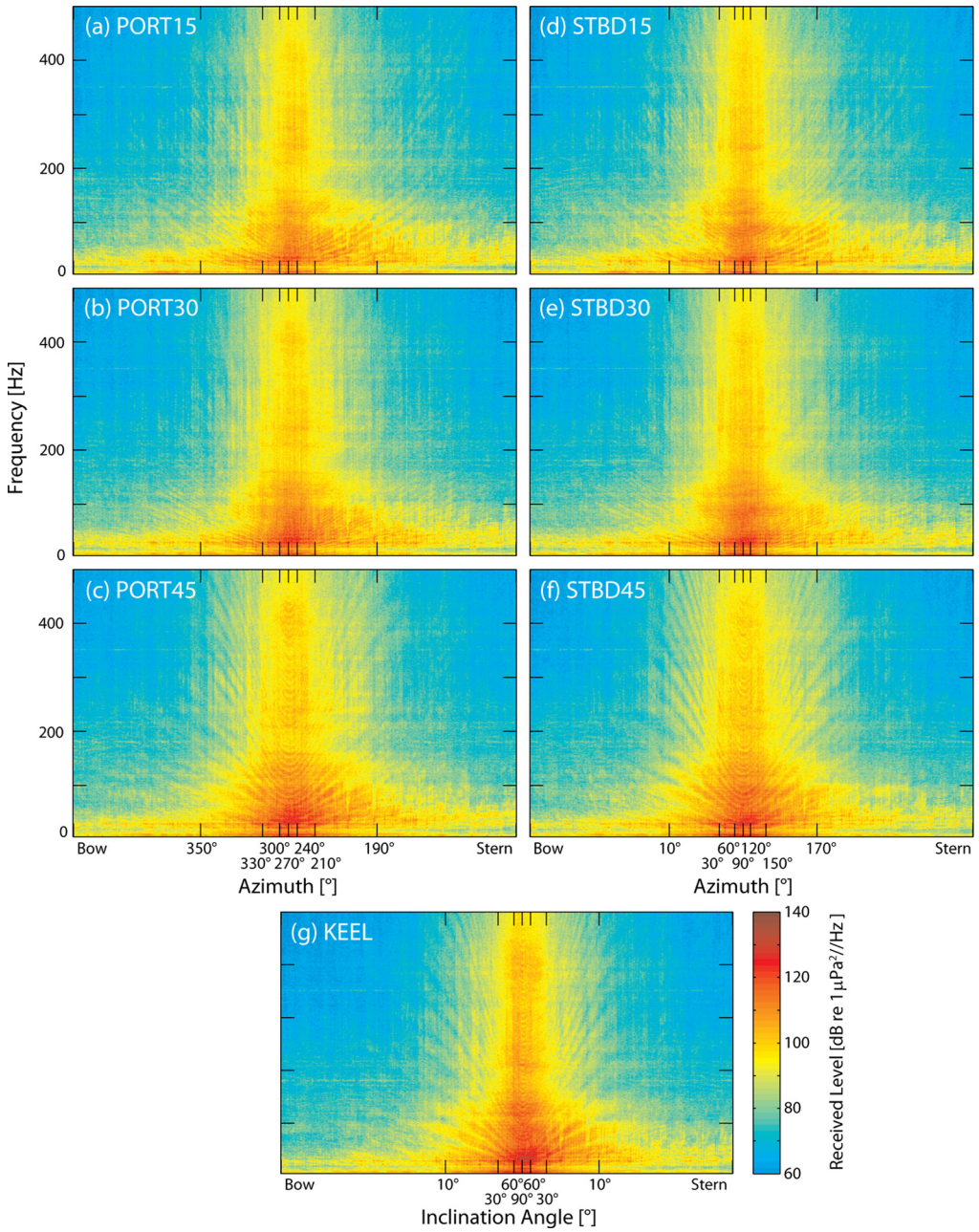

FIG. 4. (Color online) Spectrograms of underwater noise from a passage of *CSCL South China Sea* (IMO 9645920) over the hydrophone array at a speed of 20.4 knots and a draft of 9.6 m for port [(a)–(c)], starboard [(d)–(f)], and KEEL (g) aspects. Color represents sound pressure spectrum levels at the receiver in decibel (dB) relative to 1 μPa^2 for 1 Hz frequency bins with warm colors showing higher levels than cool colors. Duration of each spectrogram is 30 min starting at 8:40 GMT on January 19, 2016. Horizontal axis shows either the horizontal angle (Azimuth) or the vertical angle (Inclination Angle) from the reference point of the ship to the hydrophone at port/starboard [(a)–(f)] and KEEL (g) aspects, respectively. Spectrograms were computed from the measured pressure time series by averaging every 3 s the magnitude-squared values of five, non-overlapping FFT segments that have each a duration of 1 s.

were accounted for by using the modified Lloyd's mirror loss model [Eq. (3)]. The surface-corrected broadband (5 Hz–1 kHz) source levels for the estimated effective source depth of 3 m were 206, 209, and 202 dB re 1 μPa^2 @ 1 m for KEEL, ANSI/ISO, and Site B, respectively. Due to the increasing TL at lower frequencies of the modified Lloyd's mirror model (green lines in Fig. 3), the surface-corrected source spectra have their highest levels below 10 Hz and their maxima at the fundamental blade rate of ship propeller's at 8 Hz with 199 (KEEL), 195 (Site B), and 204 (ANSI/ISO) dB re 1 μPa^2//Hz @ 1 m [Fig. 7(b)]. In addition to the fundamental blade rate, spectral peaks occur sporadically at two series of frequencies that coincide with the harmonics of the blade ("B") and cylinder firing rate ("F") for a six-bladed propeller driven at 80 RPM by ten cylinders of the diesel engine [B and F labels in Fig. 7(a)]. The fundamental cylinder firing rate was not identifiable in the ANSI/ISO source spectra, but was present for KEEL and Site B at 12 Hz with a surface-corrected source level of 187 dB re 1 μPa^2//Hz @ 1 m. The spectral "hump" between 20 and 100 Hz that was observed as a maximum in previous studies (Arveson and Vendittis, 2000; McKenna *et al.*, 2012b) and is present in the surface-affected source spectra [Fig. 7(a)] was suppressed in the surface-corrected source spectra [Fig. 7(b)].

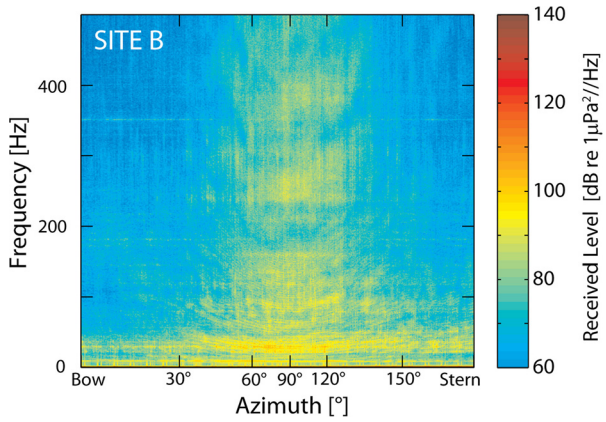

FIG. 5. (Color online) Site B spectrogram of the underwater noise from the passage of *CSCL South China Sea* (IMO 9645920). Duration of spectrogram is the same as Fig. 4, 30 min starting at 8:40 GMT on January 19, 2016.

D. Radiation patterns of the M/V SCS

Surface-affected and surface-corrected radiation patterns of the M/V SCS were computed for her fundamental blade rate (B1) at 8 Hz and the third harmonic of the diesel cylinder firing rate (F4) at 48 Hz by differencing the estimated source sound pressure levels from their respective maxima (Fig. 8). In all surface-affected radiation patterns, source sound pressure levels at beam aspect decrease with a decreasing inclination angle as expected from the directionality of the dipole that was induced by surface reflections. For example, at the STBD aspect, the surface-affected source levels decrease by 12 and 10 dB between the inclination angles of 45° and 15° for the two frequencies, respectively [Figs. 8(a) and 8(c)]. In contrast, no significant dipole component is present in the surface-corrected radiation patterns and source levels differ by only ±3 dB [Figs. 8(b) and 8(d)].

The radiation patterns of B1 exhibit both a starboard-port and a stern-bow asymmetry [Figs. 8(a) and 8(b)]. From the single, clockwise-turning propeller as viewed from aft and looking at the stern of the ship (Fig. 2), more underwater noise may be radiated at starboard and stern aspects. For example, noise levels at starboard aspect for the elevation angle of 30° are 4 dB higher than the port aspect, and on the keel are 8 dB higher at stern than the bow for an inclination angle of 60° [Fig. 8(a)]. In the radiation patterns of F4, the stern-bow asymmetry is not as pronounced as for B1 while the starboard-port asymmetry is reversed with noise levels being approximately 5 dB higher on the port than on the starboard side, in particular at the 45° port aspect.

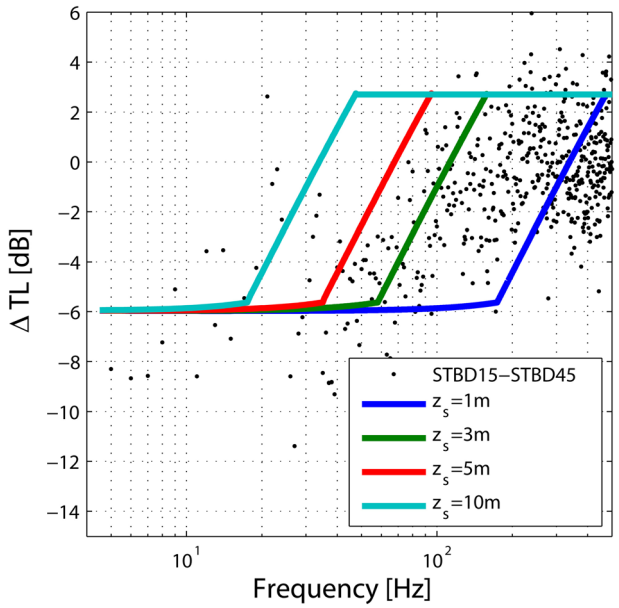

FIG. 6. (Color online) Differences in TL as a function of frequency for hydrophone pair STBD15–STBD45 at CPA during passage of *CSCL South China Sea* (IMO 9645920). TL differences computed by the modified Lloyd's mirror model are indicated by lines for source depths of 1 m (blue), 3 m (green), 5 m (red), and 10 m (cyan) with 3 m line fitting best the TL differences measured from RLs (black dots).

E. Inter-ship and speed comparison of noise levels

When compared to the M/V SCS traveling at 20.4 knots, source levels were significantly lower (up to tens of dB) for the transit of the M/V MONT at 13.4 knots (56% of her service speed) with a draft of 8.6 m and lowest for her transit at 9.5 knots (40% of her service speed) with a draft of 8.8 m (Fig. 9). While both surface-affected ANSI/ISO source level spectra of the M/V MONT peaked in the vicinity of 41 Hz at 177 dB re 1 μPa^2//Hz @ 1 m, the spectral hump extends over a wider frequency range between 20 and 100 Hz for the transit at 13.4 knots during which propeller cavitation is more developed than at 9.5 knots [Fig. 9(b)]. The hump is less pronounced in the surface-corrected source level spectrum [Fig. 9(a)].

TABLE III. Speed, draft, and environmental data during ship passages.

Name	*CSCL South China Sea*	*MSC Monterey*	
IMO	9645920	9349796	
Measurement date	January 19, 2016	January 12, 2016	January 22, 2016
SOG	20.4 knots (10.5 ms^{-1})	9.5 knots (4.9 ms^{-1})	13.4 knots (6.9 ms^{-1})
Draft [m]	9.6	8.8	8.6
Source depth [m] (acoustically derived)	3	3	3
Source depth [m] (Gray and Greeley, 1980)	3	4	4
Wind direction [degree true north]	290–264	123–135	120–102
Wind speed [ms^{-1}]	1.6–1.7	5.6–3.0	4.6–3.0
Wave height [m]	3.40–3.44	3.53–2.95	3.74–3.37
Average wave period [sec]	11.06–11.12	12.40–11.3	13.00–12.66
Mean wave direction [degree true north]	285–287	273–275	292–280

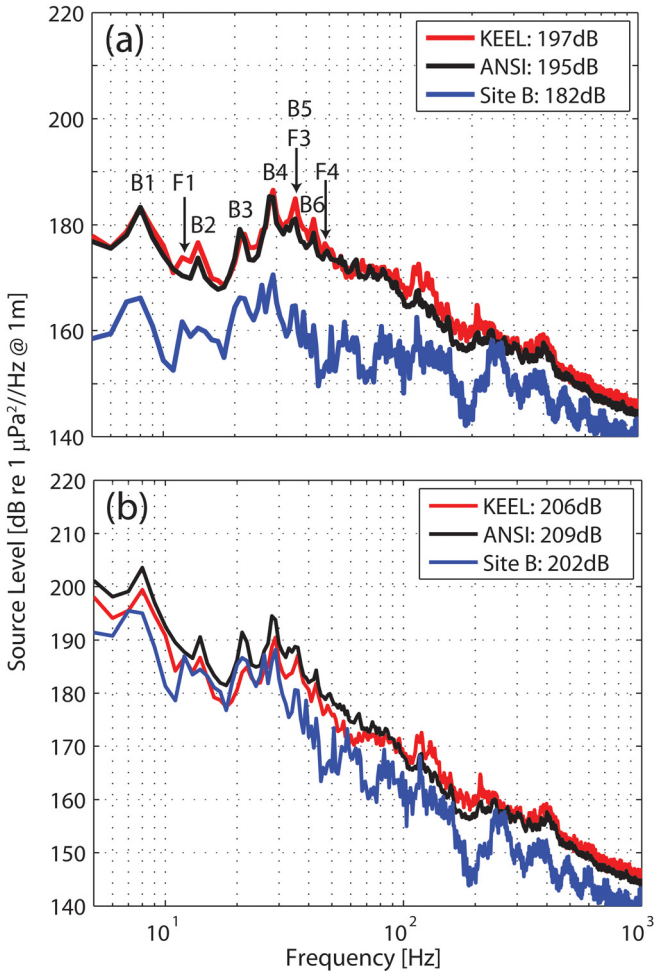

FIG. 7. (Color online) Source level spectra of *CSCL South China Sea* (IMO 9645920) at 20.4 knots and 9.6 m draft for KEEL (red), ANSI/ISO (black) and Site B (blue). (a) Source levels derived with a spherical spreading TL model, affected by interference from surface reflections. (b) Surface-corrected source levels via modified Lloyd's mirror TL model with an effective source depth of 3 m. Harmonics of blade rate and diesel cylinder firing rate are indicated in (a) by letters B and F, respectively. Fundamental blade rate (B1) is at 8 Hz.

Differences in the surface-corrected source levels for the two speeds were found to be decreasing with increasing frequency and are less than 2 dB for frequencies greater than 700 Hz. For both speeds of the M/V MONT, spectral peaks were identified at the same frequencies of 178 Hz, 360 Hz, 540 Hz, and above 1 kHz. Source levels at these frequencies for the two different speeds agreed within 2 dB. Broadband surface-corrected ANSI/ISO source levels were estimated to be 192 and 189 dB re 1 μPa^2 @ 1 m for the transits of M/V MONT at 13.4 and 9.5 knots, respectively, which is 17 to 20 dB lower than for the M/V SCS at 20.4 knots.

Surface-affected broadband source levels from Site B for both transits were 19 to 20 dB and 11 to 12 dB lower than surface-corrected and surface-affected ANSI/ISO levels, respectively.

IV. DISCUSSION

The remaining discrepancies in the surface-corrected source levels (e.g., 3 to 7 dB broadband for M/V SCS) between Site B, ANSI/ISO, and KEEL are possibly due to bottom and sea surface roughness and water column refraction effects. For example, the models could be improved further by incorporating the sea surface roughness based on the environmental data from NOAA buoy #46053 such as wind speed and wave height. However, to reproduce the detailed interference structure observed in the acoustic data more detailed knowledge of the environment, in particular characteristics of the seafloor, may need to be included as parameters to be estimated along with the source levels of the ship, e.g., Knobles (2015). This might also be helpful in verifying the decrease in TL at frequencies below 8 Hz that was predicted by the PE model based on the bottom properties from literature (Fig. 3). If the TL for frequencies below 8 Hz would indeed decrease by at least several dB, the broadband source levels (5–1000 Hz) may be overestimated by up to ~2 dB. In addition, the TL of the PE model for Site B did not suffice to compensate the observed differences in RL between the measurements in the shipping lane (ANSI/ISO and KEEL) and at Site B as it was even lower (several dB below 100 Hz) than the TL predicted by the Lloyd's mirror model [Fig. 3(c)].

The accuracy of the surface-corrected source levels computed with the modified Lloyd's mirror TL model suffers also from the assumption of a point source at a single source depth. A frequency-dependent source depth function could be helpful for reproducing the interference lobes observed in the measured data (Wales and Heitmeyer, 2002). Furthermore, uncertainty in the effective source depth can translate into significant differences of surface-corrected source levels. For example, if the uncertainty in source depth is between 1 and 5 m, the difference in TL at the lower dominant frequencies of a container ship's source spectra would be approximately 13 dB [Eq. (3)]. Hence, there is value in further improving the accuracy of the estimate for the effective source depth (function) by using a minimization or optimization algorithm that takes advantage of the spectral differences in RL between all available hydrophones that differ in elevation angle.

Despite a remaining uncertainty in source depth, the surface-corrected source levels would nevertheless be better suited for modeling of the underwater noise levels from marine traffic than the surface-affected source levels which might be strongly attenuated depending on the inclination angel(s) at which the measurements were taken. Even for the deepest possible source depth of 10 m (≈ship draft), surface-corrected source levels would be significantly higher than the surface-affected source levels at the dominant frequencies (<70 Hz) that are of interest for long-range acoustic propagation. For example, for the fundamental blade rate of 8 Hz, the surface-corrected level for a source depth of 10 m was greater by 9 dB (KEEL) to 20 dB (Site B) than the surface-affected source levels due to the modified Lloyd's mirror TL. The surface-affected source levels at Site B (McKenna *et al.*, 2012a, 2012b, 2013) may be converted into the surface-corrected source levels by compensating for the difference between the spherical spreading and modified Lloyd's TL curves as computed from Eqs. (2) and (3) and shown in Fig. 3(c) for source depths of 1, 3, and 5 m.

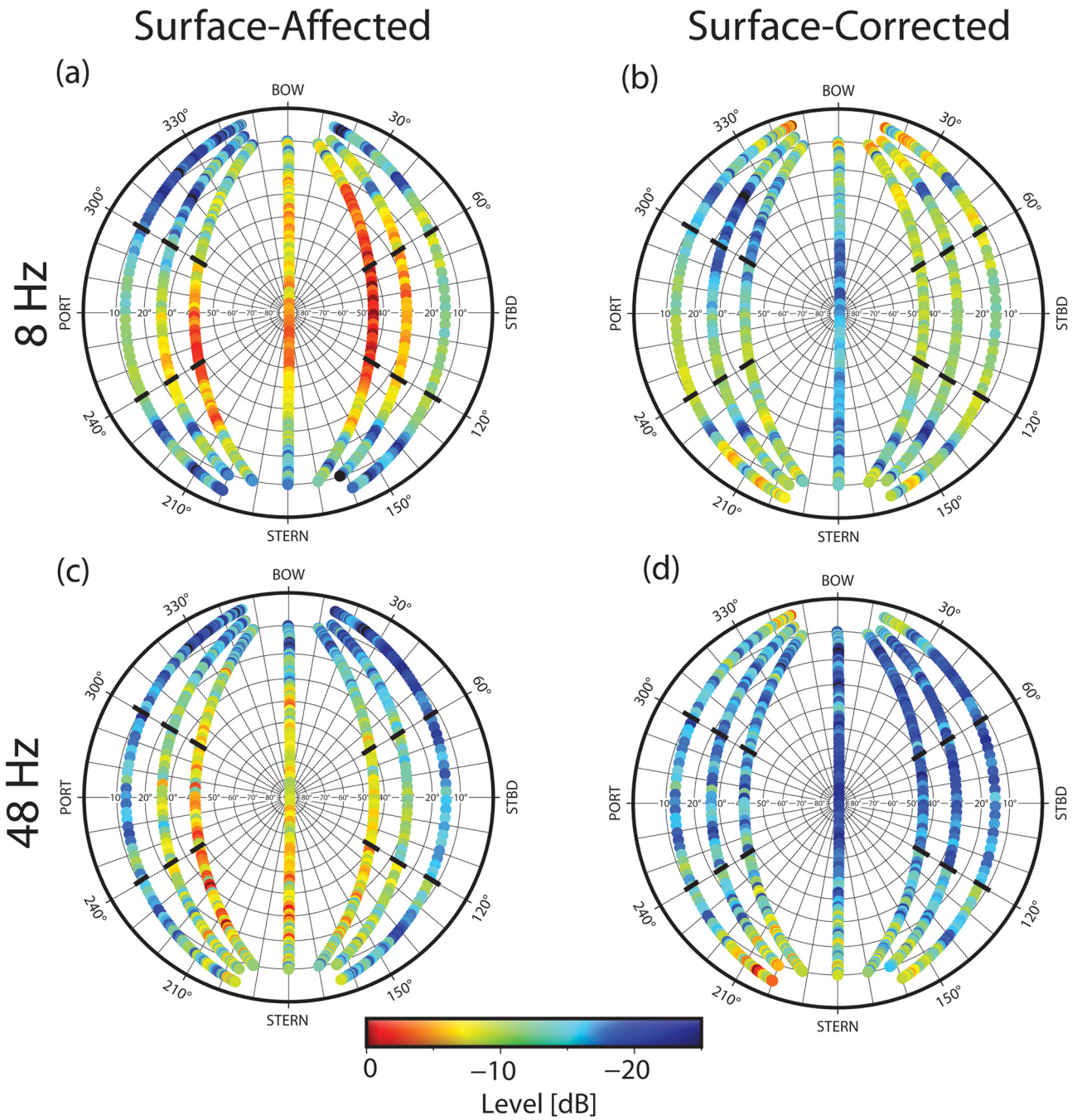

FIG. 8. (Color online) Noise radiation patterns of *CSCL South China Sea* (IMO 9645920) at 20.4 knots and 9.6 m draft for the propeller's blade rate of 8 Hz [(a) and (b)] and third harmonic of the diesel firing rate of 48 Hz [(c) and (d)]. Contributions from surface reflections in (a) and (c) (left column) were removed in (b) and (d) (right column) by a modified Lloyd's mirror TL model with a source depth of 3 m. Color represents relative source levels with respective maxima of (a) 189, (b) 224, (c) 184, and (d) 205 referenced to 1 μPa^2 at 1 m from the ship's reference point. Source levels were azimuthal-equidistantly projected onto a half-sphere from the ship's reference point that is co-located with the center of the half-sphere. Angle sectors of 60° for deriving surface-affected and surface-corrected ANSI/ISO source levels are indicated by black line segments.

The approximate compensation for the aspect-dependence of the surface-affected source levels also allows for comparisons of measurements made at different inclination angles. For example, broadband surface-affected source levels may be compared between McKenna *et al.* (2012b) and ANSI/ASA (2009) or ISO (2016) measurements by raising the source levels estimates from Site B by 11 to 13 dB. Surface-corrected broadband source levels (5–1000 Hz) may be derived from the surface-affected levels reported by McKenna *et al.* (2012b) by adding 20 to 27 dB. This might explain why the surface-affected broadband source levels reported by McKenna *et al.* (2012b) were found to be more than 15 dB lower than the source levels observed by Simard *et al.* (2016). In addition, the inclination-angle dependence of the surface-affected source levels might further explain why at an inclination angle of about 0.2° (8 m depth) (Veirs *et al.*, 2016) observed lower source levels (up to 15 dB) than McKenna *et al.* (2012b) at 10° and Arveson and Vendittis (2000) at 90° (KEEL aspect).

Surface-affected and surface-corrected source levels from single-aspect measurements at KEEL were found to be

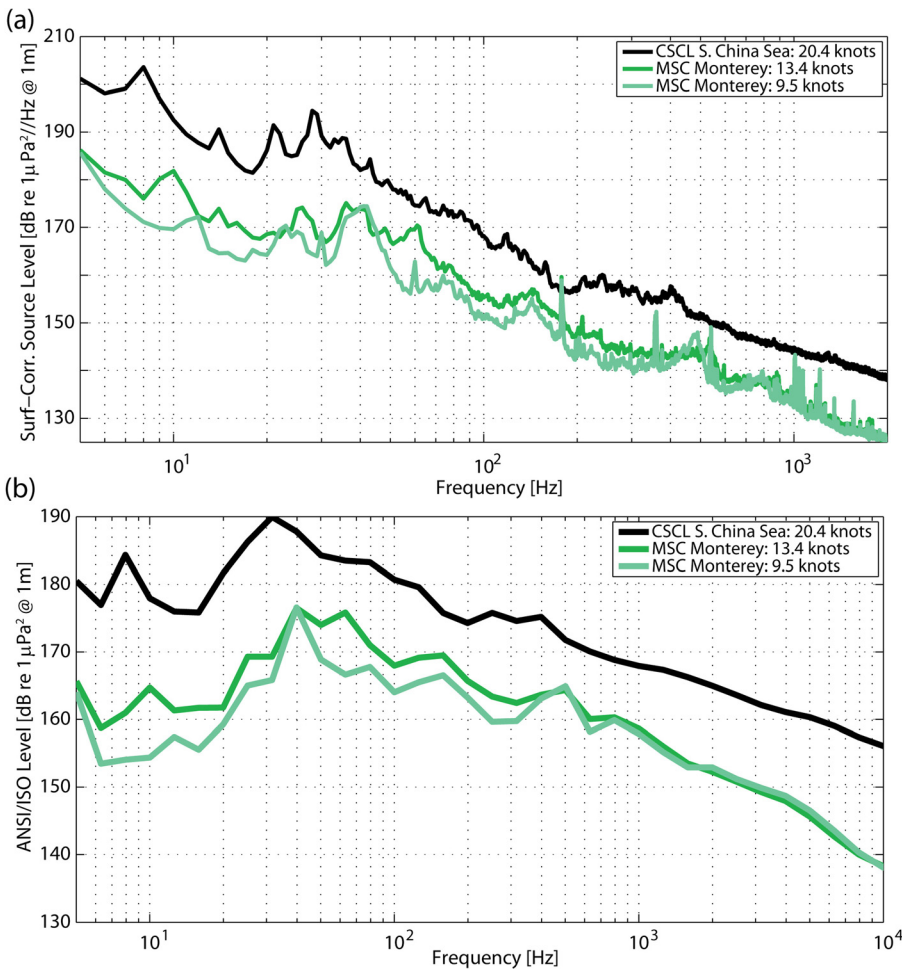

FIG. 9. (Color online) Comparison of source spectra for *CSCL South China Sea* (black line) with two transits of *MSC Monterey* (IMO 9349796) (green lines). (a) Surface-corrected (modified Lloyd's mirror) source levels were averaged over beam aspects according to ANSI/ASA (2009)/ISO (2016) for 1 Hz bins. (b) Surface-affected (spherical spreading only) ANSI/ASA (2009)/ISO (2016) levels are shown in 1/3 octave bands. Transits of *MSC Monterey*'s were at 9.5 knots and 8.8 m draft (light green lines) and at 13.4 knots and 8.6 m draft (dark green lines).

less than 6 dB higher for all frequencies when compared to the ANSI/ISO measurement while broadband source levels differed less than 2–3 dB for each of the transits. In any case, recording sound pressure levels from one site at the KEEL aspect is simpler and therefore less expensive than measuring at six sites, three different aspects on both the port and starboard sides.

ANSI/ISO signature source levels were derived from a single port and starboard measurement run due to the opportunistic approach and short period of this study. The differences in signature source levels for the two transits of the M/V MONT were attributed to the speed difference of 3.9 knots. This speed difference discourages averaging over multiple transits as required by ANSI/ASA (2009) and ISO (2016) for complete compliance and impedes a quantification of uncertainties in the signature source levels.

Radiation patterns frequently exhibited abrupt changes of up to 10 dB between consecutive source level estimates, which were neither resolved by the Lloyd's mirror TL model nor by the PE model. These variations may be suppressed by averaging over a longer time period. Harmonics for the blade rate were most easily identifiable in the ANSI/ISO source spectra, possibly due to the proximity of the ANSI/ISO receivers and the exclusion of stern aspects from the computation of KEEL source levels.

For both speeds of the M/V MONT, the ANSI/ISO signature source levels agree very well (<2 dB difference) at frequencies greater than 1 kHz in addition to the spectral peaks at 178, 360, 540 Hz (Fig. 9). This suggests that the radiated noise at these frequencies is predominately generated by auxiliary machinery, e.g., the spectral peaks might be harmonics originating from the four auxiliary generators of M/V MONT. In contrast, radiated noise at frequencies below 1 kHz differs greatly for the two speeds and hence might be generated predominately by the propulsion machinery.

V. CONCLUSIONS

Measurements of underwater radiated noise from two container ships during three passages were found to be significantly impacted by interference from sea surface reflections. When the surface reflections were accounted for by using a modified Lloyds' mirror TL model, discrepancies of up to 15 dB in broadband source levels were reduced to less than 7 dB between measurements conducted at a low inclination angle of 10° (Site B) and at the maximum inclination angle of 90° (KEEL). Therefore, the surface-corrected source levels represents a better approximation of the ships' radiated noise in the free field than surface-affected source levels, especially at frequencies at which the underwater radiated noise from the ship is most intense (<100 Hz). Modeling of underwater noise from marine traffic will benefit when surface-corrected rather than surface-affected source levels are being used in propagation models that

presuppose free-field source levels and account for sea surface interaction.

To derive surface-corrected source levels, an accurate knowledge about the *in situ* source depth(s) of the ship during her transit is necessary. In this paper, it was demonstrated that the effective source depth can be derived during a ship's transit from the spectral difference of the measured sound pressure levels at two separate inclination angles. To demonstrate the feasibility for ANSI/ASA (2009) and ISO (2016) measurement campaigns, the 15° and 45° hydrophone pair was used.

Estimates of the surface-affected ANSI/ISO signature source levels were in fair agreement (<6 dB difference) with single-aspect source levels at the maximum inclination angle of 90° (KEEL), but significantly higher (>10 dB) than source levels derived from a low inclination angle of 10° at Site B. Previously reported broadband source levels from Site B (McKenna *et al.*, 2012a, 2012b, 2013) were estimated to be significantly lower by ∼12 and ∼27 dB than their corresponding surface-affected and surface-corrected ANSI/ISO broadband source levels (5–1000 Hz), respectively.

ACKNOWLEDGMENTS

We thank Ryan Griswold, Bruce Thayre, and Rohen Gresalfi for assistance with the fieldwork as well as Erin O'Neill for help with data processing. We are also grateful for discussions with Mike Buckingham, Bill Hodgkiss, Christ de Jong, and LeRoy Dorman. This work was supported by NASA under cooperative agreement NNX14AR62A with UCSB. We thank as well Robert Miller and other members of the SBC MBON project.

ANSI/ASA (**2009**). ANSI S12.64-2009, *Quantities and Procedures for Description and Measurement of Underwater Sound from Ships–Part 1: General Requirements*" (American National Standards Institute/Acoustical Society of America, New York).

Arveson, P. T., and Vendittis, D. J. (**2000**). "Radiated noise characteristics of a modern cargo ship," J. Acoust. Soc. Am. **107**, 118–129.

Brooker, A., and Humphrey, V. (**2016**). "Measurement of radiated underwater noise from a small research vessel in shallow water," Ocean Eng. **120**, 182–189.

Carson, B., Baldauf, J. G., and Westbrook, G. K. (**1992**). "ODP Expedition: 146—Site: 893—Hole: A," http://web.iodp.tamu.edu/OVERVIEW/?&exp=146&site=893.

Collins, M. D. (**1993**). "A split-step Padé solution for the parabolic equation method," J. Acoust. Soc. Am. **93**, 1736–1742.

Cornuelle, B., Kuperman, W. A., Hodgkiss, W. S., Tippmann, J., Sarkar, J., Verlinden, C., and Sabra, K. (**2016**). "Passive travel time tomography using ships as acoustic sources of opportunity," J. Acoust. Soc. Am. **140**, 3074.

Gray, L. M., and Greeley, D. S. (**1980**). "Source level model for propeller blade rate radiation for the world's merchant fleet," J. Acoust. Soc. Am. **67**, 516–522.

Hildebrand, J. A. (**2009**). "Anthropogenic and natural sources of ambient noise in the ocean," Marine Ecology-Progress Series **395**, 5–20.

ISO (**2016**). 17208-1:2016, I. "Underwater acoustics—Quantities and procedures for description and measurement of underwater sound from ships—Part 1: Requirements for precision measurements in deep water used for comparison purposes" (International Organization for Standardization, Geneva, Switzerland).

Jansen, H. W., and de Jong, C. A. F. (**2015**). "Experimental assessment of underwater radiated sound of different ship types," in *OCEANS 2015—Genova*, pp. 1–8.

Knobles, D. P. (**2015**). "Maximum entropy inference of seabed attenuation parameters using ship radiated broadband noise," J. Acoust. Soc. Am. **138**, 3563–3575.

Kuperman, W. A., Cornuelle, B., Gemba, K. L., Hodgkiss, W. S., Sarkar, J., Tippmann, J. D., Verlinden, C. M., and Sabra, K. G. (**2017**). "A tomography experiment using ships as sources of opportunity," J. Acoust. Soc. Am. **141**, 3528.

McKenna, M. F., Katz, S. L., Wiggins, S. M., Ross, D., and Hildebrand, J. A. (**2012a**). "A quieting ocean: Unintended consequence of a fluctuating economy," J. Acoust. Soc. Am. **132**, EL169–EL175.

McKenna, M. F., Ross, D., Wiggins, S. M., and Hildebrand, J. A. (**2012b**). "Underwater radiated noise from modern commercial ships," J. Acoust. Soc. Am. **131**, 92–103.

McKenna, M. F., Wiggins, S. M., and Hildebrand, J. A. (**2013**). "Relationship between container ship underwater noise levels and ship design, operational and oceanographic conditions," Sci. Rep. **3**, 1760.

Nolet, G., and Dorman, L. M. (**1996**). "Waveform analysis of Scholte modes in ocean sediment layers," Geophys. J. Int. **125**, 385–396.

Redfern, J. V., Hatch, L. T., Caldow, C., DeAngelis, M. L., Gedamke, J., Hastings, S., Henderson, L., McKenna, M. F., Moore, T. J., and Porter, M. B. (**2017**). "Assessing the risk of chronic shipping noise to baleen whales off Southern California, USA," Endangered Species Res. **32**, 153–167.

Roquet, F., Madec, G., McDougall, T. J., and Barker, P. M. (**2015**). "Accurate polynomial expressions for the density and specific volume of seawater using the TEOS-10 standard," Ocean Modelling **90**, 29–43.

Ross, D. (**1976**). *Mechanics of Underwater Noise* (Pergamon Press, New York).

Simard, Y., Roy, N., Gervaise, C., and Giard, S. (**2016**). "Analysis and modeling of 255 source levels of merchant ships from an acoustic observatory along St. Lawrence Seaway," J. Acoust. Soc. Am. **140**, 2002–2018.

Trevorrow, M. V., Vasiliev, B., and Vagle, S. (**2008**). "Directionality and maneuvering effects on a surface ship underwater acoustic signature," J. Acoust. Soc. Am. **124**, 767–778.

Urick, R. J. (**1975**). *Principles of Underwater Sound* (McGraw-Hill, New York).

Veirs, S., Veirs, V., and Wood, J. (**2016**). "Ship noise extends to frequencies used for echolocation by endangered killer whales," PeerJ **4**, e1657.

Verlinden, C. M. A., Sarkar, J., Cornuelle, B. D., and Kuperman, W. A. (**2017**). "Determination of acoustic waveguide invariant using ships as sources of opportunity in a shallow water marine environment," J. Acoust. Soc. Am. **141**, EL102–EL107.

Wales, S. C., and Heitmeyer, R. M. (**2002**). "An ensemble source spectra model for merchant ship-radiated noise," J. Acoust. Soc. Am. **111**, 1211–1231.

Wenz, G. M. (**1962**). "Acoustic ambient noise in the ocean: Spectra and sources," J. Acoust. Soc. Am. **34**, 1936–1956.

Wessel, P., Smith, W. H. F., Scharroo, R., Luis, J., and Wobbe, F. (**2013**). "Generic mapping tools: Improved version released," EOS Trans. AGU **94**(45), 409–410.

Wiggins, S. M., Frasier, K. E., Henderson, E. E., and Hildebrand, J. A. (**2013**). "Tracking dolphin whistles using an autonomous acoustic recorder array," J. Acoust. Soc. Am. **133**, 3813–3818.

Wiggins, S. M., and Hildebrand, J. A. (**2007**). "High-frequency Acoustic Recording Package (HARP) for broad-band, long-term marine mammal monitoring," in *International Symposium on Underwater Technology 2007 and International Workshop on Scientific Use of Submarine Cables & Related Technologies 2007* (Institute of Electrical and Electronics Engineers, Tokyo, Japan), pp. 551–557.

Wittekind, D. K. (**2014**). "A simple model for the underwater noise source level of ships," J. Ship Prod. Design **30**, 1–8.